

## Article

# Model-Based Estimation of Amazonian Forests Recovery Time after Drought and Fire Events

Bruno L. De Faria <sup>1,2,\*</sup> , Gina Marano <sup>3</sup> , Camille Pioniot <sup>4</sup> , Carlos A. Silva <sup>5</sup> , Vinícius de L. Dantas <sup>6</sup>,  
Ludmila Rattis <sup>7,8</sup> , Andre R. Rech <sup>1</sup>  and Alessio Collalti <sup>9,10</sup> 

- <sup>1</sup> Programa de Pós-Graduação em Ciência Florestal, Universidade Federal Vales do Jequitinhonha e Mucuri Campus JK, Diamantina 39100-000, MG, Brazil; andre.rech@ufvjm.edu.br
  - <sup>2</sup> Federal Institute of Technology North of Minas Gerais (IFNMG), Diamantina 39100-000, MG, Brazil
  - <sup>3</sup> Department of Agriculture, University of Napoli Federico II, 80055 Portici (Naples), Italy; gina.marano@unina.it
  - <sup>4</sup> Smithsonian Tropical Research Institute, 03092 Panamá, Panama; PioniotC@si.edu
  - <sup>5</sup> School of Forest Resources and Conservation, University of Florida, Gainesville, FL 32611, USA; c.silva@ufl.edu
  - <sup>6</sup> Institute of Geography, Federal University of Uberlandia (UFU), Av. João Naves de Ávila 2121, Uberlandia 38400-902, Minas Gerais, Brazil; viniciusdantas@ufu.br
  - <sup>7</sup> Woodwell Climate Research Center, Falmouth, MA 02540, USA; lrattis@woodwellclimate.org
  - <sup>8</sup> Instituto de Pesquisa Ambiental da Amazônia, Canarana 78640-000, MT, Brazil
  - <sup>9</sup> Institute for Agriculture and Forestry Systems in the Mediterranean, National Research Council of Italy, 06128 Perugia, Italy; alessio.collalti@cnr.it
  - <sup>10</sup> Department of Innovation in Biological, Agro-food and Forest Systems, University of Tuscia, 01100 Viterbo, Italy
- \* Correspondence: blfaria@gmail.com

**Abstract:** In recent decades, droughts, deforestation and wildfires have become recurring phenomena that have heavily affected both human activities and natural ecosystems in Amazonia. The time needed for an ecosystem to recover from carbon losses is a crucial metric to evaluate disturbance impacts on forests. However, little is known about the impacts of these disturbances, alone and synergistically, on forest recovery time and the resulting spatiotemporal patterns at the regional scale. In this study, we combined the 3-PG forest growth model, remote sensing and field derived equations, to map the Amazonia-wide (3 km of spatial resolution) impact and recovery time of aboveground biomass (AGB) after drought, fire and a combination of logging and fire. Our results indicate that AGB decreases by 4%, 19% and 46% in forests affected by drought, fire and logging + fire, respectively, with an average AGB recovery time of 27 years for drought, 44 years for burned and 63 years for logged + burned areas and with maximum values reaching 184 years in areas of high fire intensity. Our findings provide two major insights in the spatial and temporal patterns of drought and wildfire in the Amazon: (1) the recovery time of the forests takes longer in the southeastern part of the basin, and, (2) as droughts and wildfires become more frequent—since the intervals between the disturbances are getting shorter than the rate of forest regeneration—the long lasting damage they cause potentially results in a permanent and increasing carbon losses from these fragile ecosystems.

**Keywords:** Amazon; recovery time; aboveground biomass; climate change; 3-PG; fire; logging



**Citation:** De Faria, B.L.; Marano, G.; Pioniot, C.; Silva, C.A.; Dantas, V.d.L.; Rattis, L.; Rech, A.R.; Collalti, A. Model-Based Estimation of Amazonian Forests Recovery Time after Drought and Fire Events. *Forests* **2021**, *12*, 8.

<https://dx.doi.org/10.3390/f12010008>

Received: 24 September 2020

Accepted: 21 December 2020

Published: 23 December 2020

**Publisher's Note:** MDPI stays neutral with regard to jurisdictional claims in published maps and institutional affiliations.



**Copyright:** © 2020 by the authors. Licensee MDPI, Basel, Switzerland. This article is an open access article distributed under the terms and conditions of the Creative Commons Attribution (CC BY) license (<https://creativecommons.org/licenses/by/4.0/>).

## 1. Introduction

Natural disturbances have a key role in forest ecosystem dynamics [1], yet global changes in climate and land-uses have intensified disturbances rates in several biomes with important consequences on the ecosystems resilience [2]. Events like droughts and wildfires are becoming widespread phenomena in vast areas of the globe, potentially affecting the ecosystem services they provide [3,4] even in humid biomes with high rainfall rates, such as Amazonia [5–7]. Housing more than half of the world's remaining rainforest

areas, Amazonian forests account for considerable carbon storage in living biomass and soils, estimated at around 150–200 Pg [8,9]. In addition, the region represents one of the most important biodiversity hotspots of the planet [10,11]. Amazonian forests are under considerable pressure due to the increased frequency and intensity of disturbances in moist tropical regions [12]. Forest fires and large-scale drought events are both directly dependent on climate [13] and their effects are expected to become more severe with climate change effects (i.e., mostly warming and reduction in precipitation). In combination with human activities, such as selective logging and other land-use changes, increasing fire and drought severity are expected to cause significant forest losses [14].

The Amazon Basin's historical baseline of disturbances has been heavily altered in the last 20 years as a result of anthropogenic activities, increasing the rates of deforestation, drought and wildfire and their impacts [15]. In the early 2000s, logging activities affected ca. 10,000–20,000 km<sup>2</sup> year<sup>-1</sup> of tropical forests in the Brazilian Amazon and it is estimated that understory fires destroyed ca. 85,000 km<sup>2</sup> of standing forests in the period 1999–2010 [16,17]. Moreover, recent studies have shown that Amazonian forests are becoming more exposed to droughts [18,19], including extreme drought events that would not be expected to take place more than once in a century (e.g., the three devastating droughts of 2005, 2010 and 2016; [20,21]). Altogether, droughts, wildfires and logging activities increase the susceptibility of forests to successive burning by increasing ignition rates, wind speed, creating drier microclimatic conditions near the soil surface and promoting exotic grass invasion. The effect of fire in forest ecosystems contrasts with that observed at larger spatial scales (i.e., global scale) and in fire-prone regions in which anthropogenic influences often reduce fire spread [22]. Therefore, the increasing risk of wildfires is an additional driver of change in the Amazon region [23].

Forest degradation due to more frequent and intense disturbances in the Amazon [24,25] results in long-term reduction in carbon stocks [26] with potential release of the C stored in Amazonian forests. The degree of degradation of the forest C stocks depends on four major factors: (1) the type of disturbance (e.g., logging, droughts and wildfires); (2) intensity (i.e., percentage of C loss); (3) the time return interval (i.e., years from one event to the next one) [25,27,28]; and (4) disturbance synergisms (i.e., the interacting effects between disturbances).

Several studies have analyzed forest recovery after disturbances at either broad or at multiple scales disturbances [29,30], but few of them have been conducted in tropical forests and specifically in the Amazon Basin. When conducted, these studies are usually limited in temporal scale (usually <20 years) [25,31,32] and focus on the effects of a single disturbance and in relatively small areas [33–35]. There is a lack of studies looking at recovery beyond 30–40 years. As a result, we still have a limited understanding on forest aboveground biomass (AGB) resilience to disturbance in Amazonian forests (i.e., how much time does it take for the forest to return to its pre-disturbance status), especially at the regional scale and taking interacting effects of multiple disturbance into consideration.

One straightforward way of addressing the consequences of disturbance in forest AGB is by integrating geospatial techniques with remote sensing and process-based forest growth models [36,37]. Specifically, remote sensing and GIS technologies allow the assessment of forest AGB at broad scales [38] whereas process-based forest growth models can provide insights on the mechanisms and processes involved in forest recovery and their relationship with spatiotemporal climate (including human)-induced scenarios. Models can help in assessing the recovery time of vegetation using climatic variables to predict vegetation productivity and its spatial variability [38]. At a regional scale, net primary productivity (NPP) is often used as an indicator of inherent plant growth potential [39]. Several studies have indeed assumed a strong relationship between productivity and biomass [40] with the first one being a function of the second. Indeed, the targeted parameter AGB is also influenced by climate, water availability and soil fertility [39–41]. In this study, we assessed the recovery time (i.e., the time necessary for a forest to recover its pre-disturbance AGB levels) of Brazilian Amazon forests AGB from drought, fire and a

combination of logging and fire disturbances, using a dynamic forest carbon model that simulates vegetation recovery time as a function of climate scenarios and geospatial data. With the present study, we aim to investigate the recovery time of AGB in the Amazon forests when subject to a disturbance caused by: (1) an extreme drought, (2) a catastrophic fire and (3) a combination of logging and fire disturbances by integrating the existing knowledge [24,42–44] within our modeling framework.

## 2. Materials and Methods

We used a spatially implicit forest productivity model based on the net primary productivity of the 3-PG model (Figure 1) (see Section 2.1 *The Model*) to estimate forest recovery time (here defined as the time necessary for a forest to recover at its pre-disturbance AGB levels). Analysis of AGB recovery was carried out for the Brazilian Amazon biome, which encompasses about 3.5 million km<sup>2</sup> located between 15° S–5° N and 40° W–80° W. The region consists of one of the largest preserved forests in the world that has been experiencing strong human disturbances in recent times, especially in “the arch of deforestation” (Figure 2).

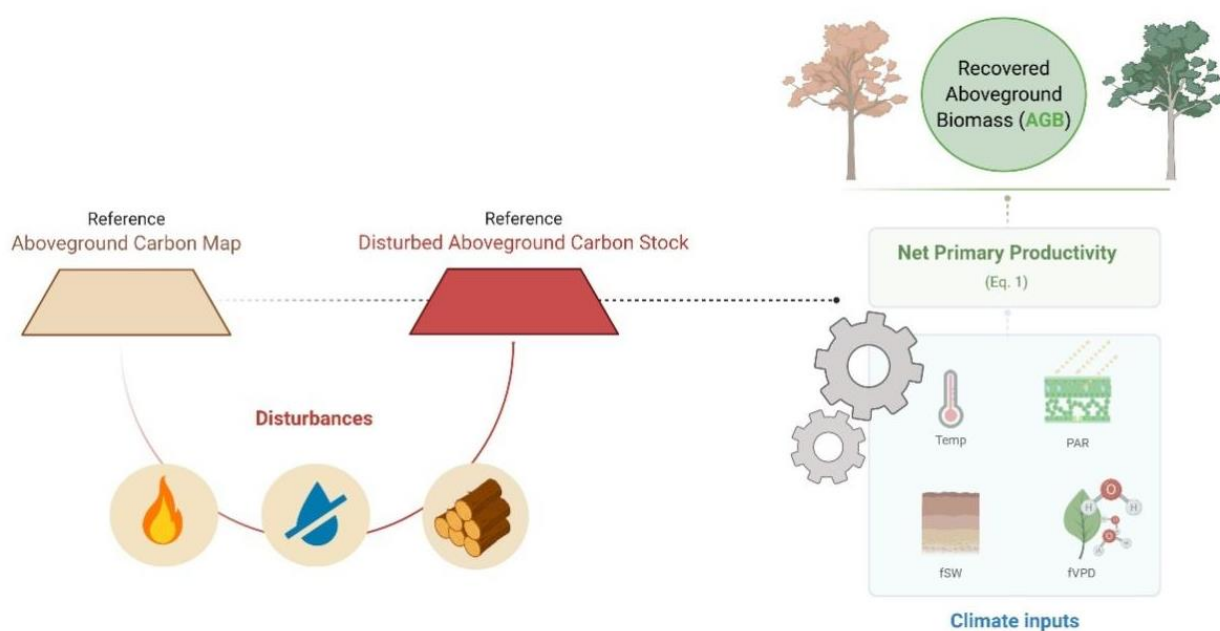


**Figure 1.** Proof-of-concept vegetation recovery time simulations as a function of climate variables (i.e., soil-plant available water ( $fSW$ ), photosynthetically active radiation (PAR), vapor pressure deficit ( $fVPD$ ), and air temperature ( $fTemp$ ), see *The Model* for description). Aboveground biomass (AGB) losses resulting from drought stress and fire are a function of the maximum climatological water deficit (MCWD, see *The Model* for description).

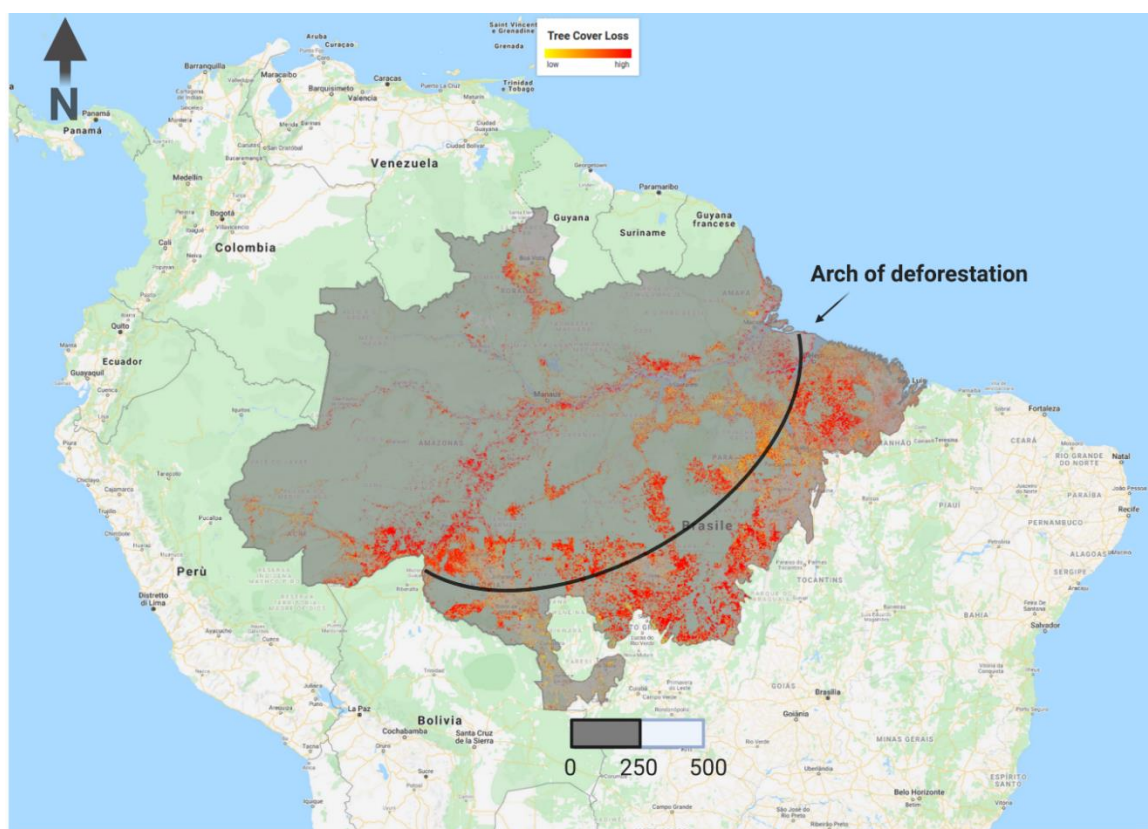


**Figure 2.** Study area: Amazonian forest in Brazil. Amazon biome extent (gray area). Forest loss map (yellow-red) has been displayed according to [45,46] (Global Forest Change dataset in Google Earth Engine). Red pixels identify areas of where tree cover loss has been detected.

### 2.1. The Model

In this study, recovery time dynamics are simulated using the 3-PG model (Physiological Principles in Predicting Growth; [47]), as embedded and parameterized into the CARLUG model by [48], driven by four monthly climatic variables: photosynthetically active radiation (PAR,  $\text{mol PAR m}^{-2} \text{ month}^{-1}$ ), vapor pressure deficit (VPD, KPa), precipitation ( $\text{mm month}^{-1}$ ) and air temperature ( $^{\circ}\text{C}$ ), respectively. The 3-PG model was used to estimate gross and net primary productivity (GPP and NPP, both in  $\text{g C m}^{-2} \text{ month}^{-1}$ ) as follows:

$$NPP = GPP \times Y \quad (1)$$

where  $Y$  is the carbon use efficiency (i.e., the fraction of GPP not used to support autotrophic respiration, known as CUE [49–51]). GPP is computed as:

$$GPP = \alpha_x \times modifiers \times PAR \times \left(1 - e^{-k \times LAI}\right) \quad (2)$$

where  $\alpha_x$  is the maximum quantum canopy efficiency (i.e., the maximum capacity in converting light into photosynthates without environmental or other functional limitations, in  $\text{mol C mol PAR}^{-1} \text{ m}^{-2} \text{ month}^{-1}$ ), *modifiers* comprise environmental limitations to maximum photosynthetic rate (temperature,  $f_{TEMP}$ ; soil water,  $f_{SW}$ ; and vapor pressure deficit,  $f_{VPD}$ ), with values ranging from zero (complete limitation) to one (no limitation). For an in-depth description of modifiers algorithms see also [48,52]. The last two terms in Equation (2) reflect the incident PAR effectively absorbed by the canopies (i.e., APAR) based on their leaf area index (LAI,  $\text{m}^2 \text{ m}^{-2}$ ) and the leaf light extinction coefficient ( $k$ , unitless) as in Beer's Law [53].

Each month, the model assumes that leaf, wood, and root carbon pools increase by an overall amount equal to the NPP, which are, respectively, allocated proportionally in their three pools as in the standard 3-PG carbon partitioning-allocation scheme [54]. The partitioning of NPP is the outcome of the climate and soil conditions interacting with vegetation through a series of differential equations that describe the flow of C within the tree compartments [48]. Therefore, the model predicts the distribution of forest biomass from carbon stocks, but in order to obtain biomass we converted C to biomass assuming that one ton of biomass contains 0.5 tons of C [55]. We assume that the re-equilibration of forest carbon after disturbances (i.e., steady state undisturbed conditions) is when the AGB growth and the decay rates stabilize. We also estimated the average time to recover 90% of old-growth forests' carbon levels. The 90% threshold has often been used in similar studies (e.g., [56]) and can thus more easily be compared to previous results; the 100% threshold corresponds to a full recovery of carbon stocks, but it may take significantly longer.

The study conducted by [48] uses the recalibrated 3-PG model parameters for the Amazonian forests (the overall parameters description and their values are shown in Supporting Information, see Table S1). The 3-PG calculates NPP as a constant fraction of GPP, using an NPP/GPP ratio ( $Y = 0.47$ ) based on empirical evidence [47]. For Brazilian Amazon forests other studies suggest  $Y$  to be closer to 0.3 [57] while others report much higher values at some tropical sites, even including Amazonian ones (i.e.,  $Y > 0.5$ ; [51]). However, the issue of whether  $Y$  is a constant value, its actual value, even including its top-down limits, is a much-debated issue as described in [51,58].

An overall 3-PG model parameter sensitivity analysis has been performed already by a number of authors (e.g., [59]) showing how the 3-PG model is mostly sensitive to stem allometric parameters (i.e., those used to obtain from trees structure the tree biomass), ratios for biomass partitioning and allocation, maximum canopy conductance, turnover time of wood, and maximum canopy quantum efficiency. For an in-depth 3-PG model parameter sensitivity analysis we refer to the works of [48,59] and this will be not considered and discussed further here. In addition, we used the pan-tropical biomass map generated by Avitabile et al. [60] as reference (pre-impact) levels to initialize the model and combining it with two comprehensive recent estimates of carbon density (i.e., estimations of [55,61] and covering a wide 250–500 Mg ha<sup>-1</sup> range (Figure S1).

## 2.2. Estimating Drought, Fire and Logging Impacts on AGB Stocks

The loss of AGB due to drought events was modeled as a function of the MCWD (Maximum Climatological Water Deficit index, representing the maximum climatological water deficit reached in the year), a common index used to measure the cumulative water stress in Amazonia (e.g., [42,62,63]). The MCWD reflects the intensity and length of the dry season, when evapotranspiration exceeds precipitation (i.e., negative balance). A measure of water deficit related to tree mortality in Amazonian forests that is denoted as in Lewis et al. [42], that is:

$$\Delta AGB = 0.378 - 0.052 \times \Delta MCWD \quad (3)$$

We estimated the MCWD anomalies (namely,  $\Delta MCWD$ ) for the year 2010 by first estimating the mean MCWD for the baseline period from 1998 to 2015, without considering both the years 2005 and 2010. The  $\Delta MCWD$  have been shown to be strong predictors of drought-associated tree mortality in the Amazon [62]. Specifically, a monthly water deficit was calculated as the difference between precipitation and evapotranspiration (with ground measurements estimated at 100 mm per month [63,64], i.e., evapotranspiration is fixed at 100 mm month<sup>-1</sup>). As a result, we assume that the forest is in water deficit when monthly precipitation falls below 100 mm. MCWD was calculated as the sum of sequential monthly water deficits, where more negative MCWD values indicate higher drought stress. We quantified the MCWD for the year of 2010 using the product 3B43 of TRMM (Tropical Rainfall Measuring Mission at 0.25° grid-resolution), and then, the average of carbon losses

for each pixel using Equation (3). The 2010 drought is one of the most intense and spatially extensive drought events ever recorded in the Brazilian Amazon [42].

Effects of wildfire were estimated by using the CARLUC-Fire model [44]. This model specifically accounts for the effects of fire by estimating forest carbon losses after a fire event as a function of its intensity (FI). FI is defined as the energy released per unit length of fire-line ( $\text{kWm}^{-2}$ ), which is a key factor in estimating how vegetation responds to fire events. The relationship between fire intensity and fire-induced biomass losses was derived from a large-scale fire experiment in southeast Amazonia [24,44] (Equation (4)). Based on this experiment, AGB losses were calculated as a function of FI as follows:

$$AGB_{losses} = \frac{1}{(1 + e^{(2.45 - 0.002373 \times FI)})} \quad (4)$$

We limit our fire analysis to areas that burned between 2003 and 2016 [65] using information at 500 m resolution from the Moderate Resolution Imaging Spectroradiometer (MODIS) Collection 6 MCD64A1 burned area product over the period 2003–2016.

As a substantial proportion of fires occurred in areas likely to have been previously logged, we accounted for this effect in the estimation of the initial AGB by incorporating an additional loss in fire effects of 40% in burned areas that were also cleared. We assumed this based on findings of Berenguer et al. [43] that an average forest under selective logging stores about 40% less carbon. Logged areas were defined using data from the annual Landsat-based Project for Monitoring Amazonian Deforestation (PRODES, <http://www.obt.inpe.br/prodes>). Because edge effects from logging have been shown to affect forests up to 2–3 km from the border [66], we include forests located within 3 km from a deforested pixel, as a selective logging influence zone and they were defined using data from PRODES with cumulative deforestation up to 2017.

### 2.3. Experimental Runs

We ran the 3-PG model at  $3 \text{ km} \times 3 \text{ km}$  spatial resolution under mean monthly climate conditions for the 1980–2009 period, to estimate the forest recovery time for both drought, fire and logging + fire impacts (includes loss from logging and losses from fire). Climate input variables used to calculate the climatic means consisted of monthly series of temperature and mean vapor pressure deficit from the Climate Research Unit (CRU TS; [67]), while PAR was obtained from the GOES–9 satellite product [68]. In each pixel, AGB recovery was assessed by simulating AGB dynamics with the model after an AGB loss corresponding to disturbance impact.

### 2.4. Assessing Model Results

Light detection and ranging (Lidar) remote sensing is widely used for monitoring forest structure and biomass dynamics [69,70] in many forest ecosystems [71]. For instance, airborne lidar (ALS) technologies help quantify changes in canopy structure, carbon stocks and recovery time at the local-to-regional scale under different types of forest degradation (e.g., [25,72,73]).

In the present study, we compare our modeled recovery time from fire in logged areas with airborne lidar-derived aboveground carbon density (ACD) recovery estimates in forest stands (2891.45 Ha) located in Feliz Natal (Mato Grosso, Brasil) that were logged and burned once. For computing the recovery time of ACD from lidar, we applied a model developed by Rappaport et al. [25] that used multiple linear regression to model the recovery time of ACD ( $\text{Kg C m}^{-2}$ ) in degraded forest stands based on degradation type. In their study, the model was calibrated using a chronosequence of ACD maps derived from lidar and degradation history data (from 2013 to 2018) across degraded forests stands [25]. The model is presented in Equation (5) and shows adjusted  $R^2$  of 0.89. Herein, we chose to

compare our results with those provided in Rappaport et al. [25] due to lack of available field data on the time scale addressed here to assess recovery time.

$$RT = 62.259 + 11.395 \times \log(t) - 10.268 \times CF1 \quad (5)$$

where RT refers to recovery time, t refers to time (years) and CF1 refers to degradation history, once-burned stands.

### 2.5. Disturbance Return Interval

In order to inquire whether global changes could determine an increase in future drought and fire frequency we projected the areal extent and spatial patterns of future drought and fire impacts up to the year 2100 in order to understand whether global changes could determine an increase in future drought and fire frequency in the study area. We analyzed both future precipitations (based on Representative Concentration Pathways, i.e., RCP 8.5—representing unmitigated climate change scenario) and a land use changes scenario (based on Aguiar et al. [74]) with a decrease in the extension and level of protection of the areas and increases in deforestation rates from 2014 to 2020 and continuing until 2100.

We built drought scenarios (2040–2070 and 2071–2100) using precipitation (related with water stress, MCWD) from the ensemble of 35 climate models participating in the Coupled Model Intercomparison Project phase 5 (CMIP-5, [75]). In detail, we derived the forcing from the mean monthly simulated precipitation anomalies first averaged for all 35 models and then bias corrections with Tropical Rainfall Measuring Mission (TRMM data product 3B43 [63]). To investigate frequency of future Amazonian droughts we assumed severe drought condition when MCWD anomalies (subtraction between future projections and the historical average) is  $< -40$  mm (threshold derived by Phillips et al. [62]), below this threshold water stress is assumed to induce losses in AGB. We also used maps of predicted change in fire recurrence in response to global changes obtained from Fonseca et al. [76] based on future land-use change data by Aguiar et al. [74]. The fire scenarios (2040–2070 and 2071–2100) developed by Fonseca et al. [76] combine the effects of future land-use and climate change on fire relative probability in the Brazilian Amazon in the best-case and worst-case scenarios. We assume fire relative probability to equal fire relative frequency and then determine the mean fire return interval as the inverse of fire relative frequency.

## 3. Results

Results show that disturbances have substantially affected biomass in Brazilian Amazonia. In the locations affected by drought, fire and logging + fire, AGB decreased by 4%, 19% and 46%, respectively (Figure 3). Our results suggest that during the 2010 drought, about 1.5 million km<sup>2</sup> of the Brazilian Amazon lost a considerable amount of AGB (we considered losses  $\geq 10\%$  of the initial AGB). Fire could also produce substantial losses in above-ground carbon affecting 550,000 km<sup>2</sup> especially in southern Brazilian Amazon. Approximately 150,000 km<sup>2</sup> of the burned forest patches were located within 3 km from a logged forest.

Average AGB recovery time was 27 years for drought-impacted, 44 years for burned, and 63 years for logged + burned areas (includes loss from logging and loss from fire). Recovery time from drought revealed a northwest-to-southeast gradient in the study area (Figure 4a). Roughly 20% of these drought-affected areas, corresponding to ca. 364,000 km<sup>2</sup>, were estimated to recover in the first 10 years, with maximum values reaching 90 years in parts of southeastern Brazilian Amazonia (Figure 4). Forest fires were widespread across the “arch of deforestation” (the region in southern and eastern Amazonia where the rates of deforestation are higher) during the period 2003–2016 (Figure 4b). The longest recovery times during this period were concentrated along the eastern and southwestern extent of Amazon forests in Brazil, where the maximum was about 150 years after fire disturbance. Subsequent wildfires events (i.e., multiple fires in the same location) accounted for 10% of all forest fires during the period 2003–2016, delaying forest recovery times within these

areas (Figure 4b). The longest recovery times were found in logged-and-burned forests with maximum values reaching 184 years (Figure 4c,c1). These results consider a recovery of the carbon stock corresponding to 100% (i.e., recovery time ~184 years) (see *The Model*) resulting in a difference of about 122 years in logged and burned forest which would be much faster if we would consider a recovery threshold of 90% (i.e., recovery time ~62 years) (Figure S2).

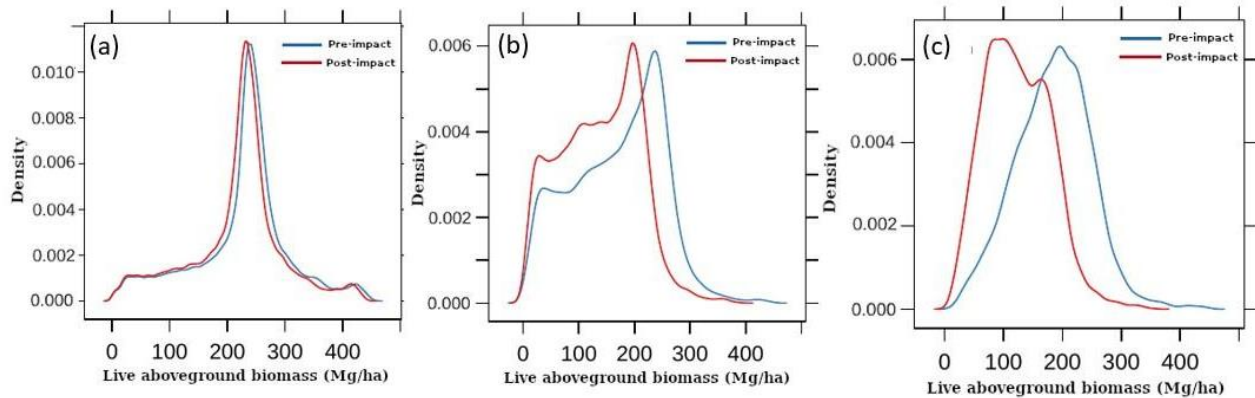


**Figure 3.** Biomass density plots describing patterns before and after drought (a), fire (b) and logging + fire (c) impacts. Only areas that burned between 2003 and 2016 are considered and, for (c), only burned areas up to 3 km from logging areas. Recovery is defined as 100% of pre-disturbance AGB.

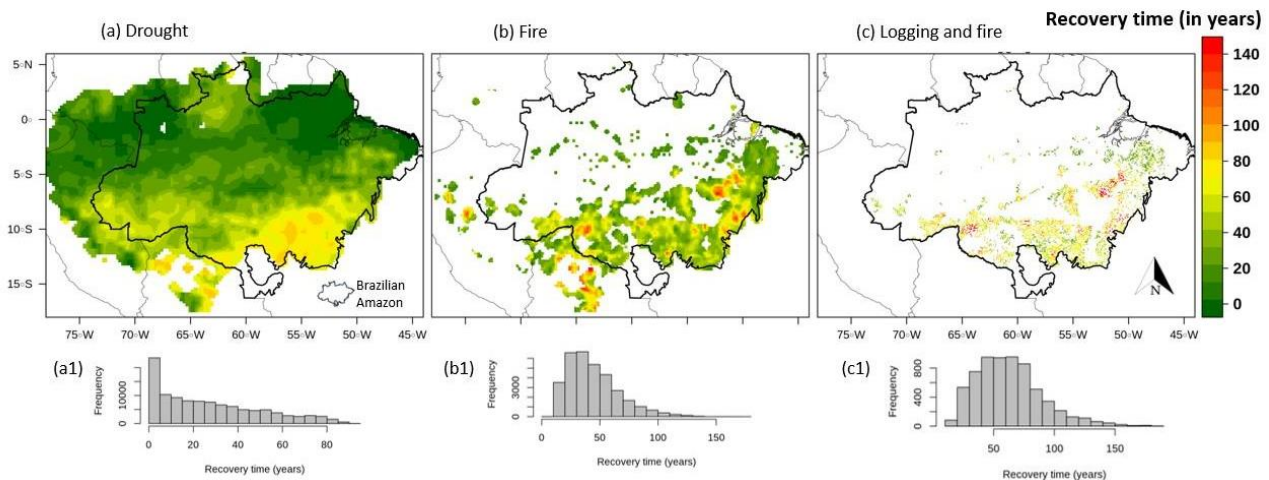


**Figure 4.** Aboveground recovery time (in years) for 2010 drought (a), fire areas that burned between 2003 and 2016 (b) and in areas that were both burned and logged (c). Histogram plots summarize AGB recovery pixels distributions (in years), for drought (a1), fire (b1) and logging + fire (c1).

We compared our results with a lidar-derived model of recovery time in stands that were logged and burned once (Figure 5a). Our estimations show smaller AGB decreases in comparison with lidar-based estimates of carbon losses from fire (loss of AGB of 46% vs. 55%). However, recovery rates were shown to be strongly correlated (Figure 5b).

Increases in the extent and frequency of drought and fire (Figure 6) suggest that these future disturbances could undermine the full forest recovery. Our results suggest that by 2070 the area affected by drought will increase approximately three-fold (Figure 6—top panel). Moreover, from the middle to the end of the century, the mean fire return intervals (FRI) was projected to decrease from 10 to 8 years and the median FRI to decrease from 8 to 6 years from the 2040–2070 period to the 2070–2100 periods, respectively, in a worst case

land use change scenario (Figure 6 bottom panel). However, in a more optimistic scenario the area subject to high fire frequency would be smaller (Figure 6 middle panel).

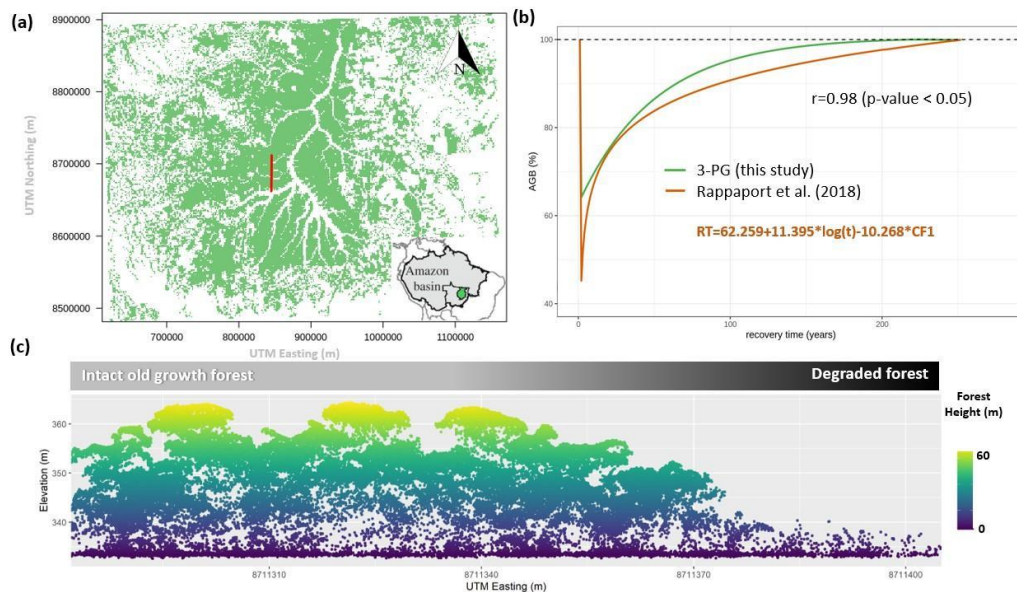


**Figure 5.** Airborne light detection and ranging (lidar) data were sampled (red line) in Feliz Natal, within the Xingu basin (light green), Brazilian state of Mato Grosso (a). The forest growth model (3-PG green line) shows the relationship between aboveground biomass (%) and recovery time in years. We compared it with a lidar-derived model of recovery time in stands that were logged and burned once (CF1 refers to once-burned) [25] (orange line) (b). A sample of vertical profile of a recovering forest which was degraded by fire and selective logging (c). The discrete return lidar data used for creating the transect figure were acquired in 2018 with a point density of  $22.98 \text{ points m}^{-2}$  covering an area of 2891.25 ha in Feliz Natal, Mato Grosso, Brazil [25], as part of the Sustainable Landscapes Brazil project program (data available from: <https://www.paisagenslidar.cnpqia.embrapa.br/webgis/>; details of airborne lidar (ALS) data acquisitions are presented in the supplementary material, Table S2).

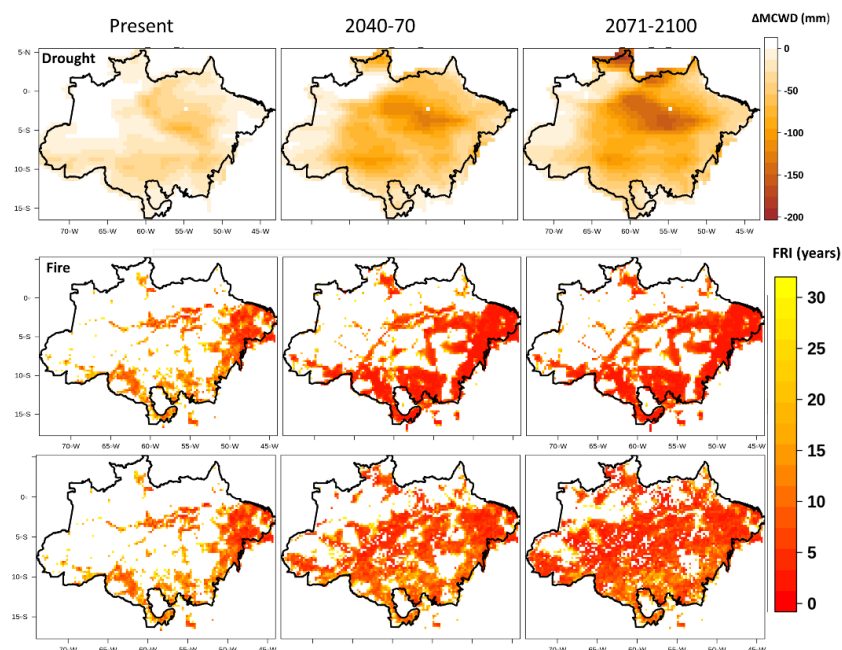


**Figure 6.** Projected changes in droughts (as maximum climatological water deficit anomalies,  $\Delta\text{MCWD}$ ) (upper panel) and fire return interval based on an optimistic land use scenario (mid panel) and in the unmitigated scenarios with the worst-case land-use scenario (bottom panel).

#### 4. Discussion

In the present study, we explored the AGB changes after drought, fire and a combination of logging and fire disturbances and the time needed for complete recovery as a function of both climatic conditions and AGB in the Brazilian Amazon forest, using a modeling-based approach. Our results suggest that fire is a much greater threat than drought for the forest resilience, especially if logging occurs. These results highlight the key threat imposed by fire to Amazon forests. The intensity of the disturbance event is strongly related to both the amount of AGB lost and the recovery time of the forest. The biomass recovery rates estimates reported here are consistent with those from Poorter et al. [56] that showed AGB of Neotropical second growth forest took a median time of 66 years to recover to 90% of previous growth values after multiple disturbances events, including land use changes. On the other hand, recent evidence [77] suggests that recovery time might take at least 150 years until secondary forests (re)gain carbon levels similar to primary forests, after drought disturbances thus indicating that these biomes have recovery rates that are much lower than previously suggested.

Our results also suggest that by the end of the century, especially after 2070, the Brazilian Amazon will be affected by more frequent droughts with the southern area being more vulnerable since it will need a longer time to recover after these events. Thus, climate change will greatly increase the threat imposed to the forest, potentially jeopardizing forest resilience. The interplay between longer forest recovery times and more frequent droughts has been previously evidenced in the Amazonia, where longer recovery times have been documented [78]. Moreover, if on the one hand the extreme droughts of 2005, 2010 and 2016 have prevented the full recovery of the forests, on the other, drought effects on forest canopy carbon fixation capacity could potentially persist for several years during recovery processes [78], leading to forest degradation and changes in forest species composition, and evidence suggests that taller tree species have significantly higher mortality than small tree species, when subject to drought [79,80].

Our findings also confirm that the land carbon sink in the Brazilian Amazon will be strongly impacted by a regime of a chronic state of incomplete recovery [78], with adverse consequences also on the GPP due to shifts in precipitation patterns caused by anthropogenic emissions [81–83]. Indeed, across Amazon forests, GPP is modeled to decrease linearly with increasing seasonal water deficit [82]. Longer and more intense dry seasons have been forecasted, together with an increased frequency and severity of drought events [84–86] and future Amazon droughts are expected to become even more frequent [87,88]. Our projections suggest about one extreme drought per decade (drought return interval ranging from 4 to 16 years depending on the scenario of climate change). If drought frequency increases, Amazon forest, both as species composition and regional carbon sink, will be affected, which will thereby have an impact on global carbon cycling and contribute further to climate change [62,80,89,90]. Previous studies have shown increased fire occurrence and tree mortality during and after Amazon droughts [6,89,91–93]. If these events continue to increase in frequency, large parts of the Amazon could potentially shift from rainforest vegetation to a fire-maintained degraded forest and may promote the persistence of degraded forests with a savanna-like structure [94,95]. This change in forest type, structure and ecology would most likely reduce both the forest sink capacity and even its biodiversity and ecosystem services [94]. The net increase in areas that are more susceptible to wildfires, induced by either drought events increase, or potentially intensified by climate change, could lead to significant biomass losses [9,96].

Human pressures play a crucial role in fire ignitions, wildfires could break out also in non-dry years as in 2019, when more than 69,000 km<sup>2</sup> burnt despite the absence of anomalous drought [97]. As droughts and wildfires are expected to become more frequent, the time of occurrence between these disturbances may even get shorter than forest recovery time, determining permanently damaged ecosystems and widespread degradation [95]. Although forest growth models are powerful tools that can be applied in simulating the C dynamics in forests [98,99], our results are subject to some uncertainty and a number

of caveats [100,101]. In this study, we modeled vegetation recovery time as a function of climate only. This approach does not account for regional variation in growth rates depending on soils types (due to their inner physico-chemical properties such as water retention or local-scale variation based on prior land use [92,93]) growth rates are also known to vary significantly by species [43]. In addition to the mechanisms mentioned above, CO<sub>2</sub> fertilization of Amazonian vegetation and nitrogen deposition could play an important, but yet often neglected, role in forest regeneration [102]. It has also been suggested that atmospheric CO<sub>2</sub> generally stimulates plant growth with increased rates in photosynthetic activity and indirectly through increased water-use efficiency [103], but not in all cases [104]. As CO<sub>2</sub> accumulates in the atmosphere, Amazonian trees may also accumulate more biomass resulting in denser canopies and faster growth [105]. But an increased atmospheric CO<sub>2</sub> concentration necessarily implies an increase in mean air temperature which is in turn speculated to increase plants' respiration and should result in a levelled-off forest carbon use efficiency [83]. Recent studies indicate that the ability of intact tropical forests to remove carbon from the atmosphere may be already saturating [9,106] while others indicate for tropical species higher thermal acclimation capacities to buffer C-losses by respiration [51], thus, calling for more studies on the possible consequences of warming and increased atmospheric CO<sub>2</sub> concentration on forest dynamics. However, in the Amazon phosphorus is an important limiting nutrient over large parts and its low availability may limit positive CO<sub>2</sub> fertilization effects.

#### *Future Possibilities for Model Improvement*

Lidar-derived 3D-point cloud and biomass products can be used to enhance models' representation of complex and heterogeneous forest ecosystems, such as those found in Amazonia [107], and therefore can be used as input or to initialize vegetation models [108]. For instance, Longo et al. [109] have used lidar to obtain initial conditions for an ecosystem model that requires an initial state for forest structure. Their method to derive the vertical structure of the canopy from high-resolution airborne lidar successfully characterized the diversity of forest structure variability caused by human-induced forest degradation (such as logging and fire).

This new approach has strong implications on modeling recovery time and the successional trajectories of the Amazonian disturbed forest because it does not require any assumption on the successional stage of the forest, but only the vertical distribution of returns. Moreover, it could be adapted to space-borne lidar data, including NASA's Global Ecosystem Dynamics Investigation (GEDI, [110]). Fusion of GEDI and optical data [111] will further expand the spatial extent of available lidar data and potentially provide tools capable of mapping drought, fire and logging impacts helping models to assess recovery time. Moreover, integration of GEDI with either optical or radar [112] wall-to-wall data could allow large-scale characterization of forest ecosystems structure providing accurate measurements of biomass stock that could be used for assessing recovery time via repeated measurements.

## **5. Conclusions**

This study shows how forest growth models can be used as tools for complementing field-based studies on recovery time by investigating the spatial and temporal dynamics and processes of forest recovery. Indeed, our biomass recovery map illustrates both spatial and climatic variability in carbon sequestration potential due to forest re-growth. By mapping potential for biomass recovery across Amazonia, policy makers could focus their efforts on specific areas that require special protection and need to be preserved. Moreover, such recovery maps could also help by identifying areas with higher carbon sequestration potential thus supporting policies and concrete actions to mitigate forest degradation in areas where biomass resilience is under increasing stress (such as southeastern Amazonia). The capability and timing of forest recovery after drought, fire and logging are urgent and hot topics for applied research calling upon conservation and policy actions in Amazonia.

Future changes in fire regimes could push some Amazonian regions into a permanently drier climate regime and weaken the resilience of the region to possible large-scale drought–fire interactions driven by climate change. We are far from an integrated view of forest recovery processes, yet the results presented in this study may provide some new insights about forest recovery time after disturbances. The consequences that an extreme climatic event, such as a drought, may cause in the forest can result in a net loss of ecosystem services compromising these ecosystems dynamics in the long term. As a major result of projected increases in fire and drought frequency and intensity in the region, Amazonian forest resilience appears, in the medium and long term, to be severely jeopardized.

**Supplementary Materials:** The following are available online at <https://www.mdpi.com/1999-4907/12/1/8/s1>. Figure S1. Pre-disturbance reference biomass map [44]. Figure S2. The ABG dynamic as reproduced by the forest growth model (3-PG green line) showing the relationship between aboveground biomass (%) and recovery time in years to reach recovery threshold. Red dotted line 90% threshold and black dotted line 100% threshold. Table S1: Parameters description and their values used in 3-PG model (modified from Hirsch et al., [48]). Table S2: Details of ALS data acquisitions.

**Author Contributions:** Conceptualization, B.L.D.F.; methodology, B.L.D.F., A.C. and C.P.; software, B.L.D.F. and C.A.S.; draft preparation, G.M., A.C., B.L.D.F., C.P., L.R., V.d.L.D. and A.R.R.; writing—review and editing, G.M., A.C., C.P., L.R., C.A.S., V.d.L.D., B.L.D.F. and A.R.R.; visualization, B.L.D.F., C.A.S. and G.M.; supervision, G.M., A.C. and A.R.R. All authors have read and agreed to the published version of the manuscript.

**Funding:** This research received no external funding.

**Acknowledgments:** B.L.D.F. would like to thank the IFNMG and CNPq for financial support. He would like to especially thank the IFNMG campus Pirapora for giving him the opportunity to pursue a PhD. A.R.R. and B.L.D.F. thanks the support received from PPGCF/UFVJM.

**Conflicts of Interest:** The authors declare no conflict of interest.

## References

- Seidl, R.; Fernandes, P.M.; Fonseca, T.F.; Gillet, F.; Jönsson, A.M.; Merganičová, K.; Netherer, S.; Arpaci, A.; Bontemps, J.D.; Bugmann, H.; et al. Modelling natural disturbances in forest ecosystems: A review. *Ecol. Model.* **2011**, *222*, 903–924. [CrossRef]
- D’Andrea, E.; Rezaie, N.; Prislán, P.; Gričar, J.; Collalti, A.; Muhr, J.; Matteucci, G. Frost and drought: Effects of extreme weather events on stem carbon dynamics in a Mediterranean beech forest. *Plant Cell Environ.* **2020**, *43*, 2365–2379. [CrossRef] [PubMed]
- Pyne, S. The Ecology of Fire. Available online: <https://www.nature.com/scitable/knowledge/library/the-ecology-of-fire-13259892/> (accessed on 10 June 2020).
- Noce, S.; Collalti, A.; Valentini, R.; Santini, M. Hot spot maps of forest presence in the Mediterranean basin. *IForest* **2016**, *9*, 766–774. [CrossRef]
- Mishra, A.K.; Singh, V.P. A review of drought concepts. *J. Hydrol.* **2010**, *391*, 202–216. [CrossRef]
- Brando, P.M.; Nepstad, D.C.; Davidson, E.A.; Trumbore, S.E.; Ray, D.; Camargo, P. Drought effects on litterfall, wood production and belowground carbon cycling in an Amazon forest: Results of a throughfall reduction experiment. *Philos. Trans. R. Soc. B Biol. Sci.* **2008**, *1498*, 1839–1848. [CrossRef]
- Leskinen, P.; Cardellini, G.; González García, S.; Hurmekoski, E.; Sathre, R.; Seppälä, J.; Smyth, C.E.; Stern, T.; Verkerk, H. Substitution effects of wood-based products in climate change mitigation. *From Sci. Policy* **2018**, *7*, 28.
- Mitchard, E.T.A.; Feldpausch, T.R.; Brienen, R.J.W.; Lopez-Gonzalez, G.; Monteagudo, A.; Baker, T.R.; Lewis, S.L.; Lloyd, J.; Quesada, C.A.; Gloor, M.; et al. Markedly divergent estimates of Amazon forest carbon density from ground plots and satellites. *Glob. Ecol. Biogeogr.* **2014**, *23*, 935–946. [CrossRef]
- Brienen, R.J.W.; Phillips, O.L.; Feldpausch, T.R.; Gloor, E.; Baker, T.R.; Lloyd, J.; Lopez-Gonzalez, G.; Monteagudo-Mendoza, A.; Malhi, Y.; Lewis, S.L.; et al. Long-term decline of the Amazon carbon sink. *Nature* **2015**, *519*, 344–348. [CrossRef]
- Saatchi, S.; Houghton, R.A.; Dos Santos Alvalá, R.C.; Soares, J.V.; Yu, Y. Distribution of aboveground live biomass in the Amazon basin. *Glob. Chang. Biol.* **2007**, *13*, 816–837. [CrossRef]
- Gardner, T.A.; Barlow, J.; Chazdon, R.; Ewers, R.M.; Harvey, C.A.; Peres, C.A.; Sodhi, N.S. Prospects for tropical forest biodiversity in a human-modified world. *Ecol. Lett.* **2009**, *12*, 561–582. [CrossRef] [PubMed]
- Lewis, S.L.; Edwards, D.P.; Galbraith, D. Increasing human dominance of tropical forests. *Science* **2015**, *349*, 827–832. [CrossRef]
- Seidl, R.; Schelhaas, M.J.; Lexer, M.J. Unraveling the drivers of intensifying forest disturbance regimes in Europe. *Glob. Chang. Biol.* **2011**, *17*, 2842–2852. [CrossRef]

14. Malhi, Y.; Aragão, L.E.O.C.; Galbraith, D.; Huntingford, C.; Fisher, R.; Zelazowski, P.; Sitch, S.; McSweeney, C.; Meir, P. Exploring the likelihood and mechanism of a climate-change-induced dieback of the Amazon rainforest. *Proc. Natl. Acad. Sci. USA* **2009**, *106*, 20610–20615. [[CrossRef](#)] [[PubMed](#)]
15. Exbrayat, J.F.; Liu, Y.Y.; Williams, M. Impact of deforestation and climate on the Amazon Basin's above-ground biomass during. *Sci. Rep.* **2017**, *7*, 1–7. [[CrossRef](#)] [[PubMed](#)]
16. Morton, D.C.; Le Page, Y.; DeFries, R.; Collatz, G.J.; Hurtt, G.C. Understorey fire frequency and the fate of burned forests in southern Amazonia. *Philos. Trans. R. Soc. B Biol. Sci.* **2013**, *368*, 20120163. [[CrossRef](#)] [[PubMed](#)]
17. Asner, G.P.; Knapp, D.E.; Broadbent, E.N.; Oliveira, P.J.C.; Keller, M.; Silva, J.N. Ecology: Selective logging in the Brazilian Amazon. *Science* **2005**, *310*, 480–482. [[CrossRef](#)] [[PubMed](#)]
18. Stocker, B.D.; Zscheischler, J.; Keenan, T.F.; Prentice, I.C.; Seneviratne, S.I.; Peñuelas, J. Drought impacts on terrestrial primary production underestimated by satellite monitoring. *Nat. Geosci.* **2019**, *12*, 264–270. [[CrossRef](#)]
19. Brodribb, T.J.; Powers, J.; Cochar, H.; Choat, B. Hanging by a thread? Forests and drought. *Science* **2020**, *368*, 261–266. [[CrossRef](#)] [[PubMed](#)]
20. Jiménez-Muñoz, J.C.; Mattar, C.; Barichivich, J.; Santamaría-Artigas, A.; Takahashi, K.; Malhi, Y.; Sobrino, J.A.; Schrier, G. Van Der Record-breaking warming and extreme drought in the Amazon rainforest during the course of El Niño 2015–2016. *Sci. Rep.* **2016**, *6*, 33130. [[CrossRef](#)] [[PubMed](#)]
21. Marengo, J.A.; Espinoza, J.C. Extreme seasonal droughts and floods in Amazonia: Causes, trends and impacts. *Int. J. Climatol.* **2016**, *36*, 1033–1050. [[CrossRef](#)]
22. Nepstad, D.C.; Stickler, C.M.; Soares-Filho, B.; Merry, F. Interactions among Amazon land use, forests and climate: Prospects for a near-term forest tipping point. *Philos. Trans. R. Soc. B Biol. Sci.* **2008**, *363*, 1737–1746. [[CrossRef](#)] [[PubMed](#)]
23. Marengo, J.A.; Souza, C.M.; Thonicke, K.; Burton, C.; Halladay, K.; Betts, R.A.; Alves, L.M.; Soares, W.R. Changes in Climate and Land Use Over the Amazon Region: Current and Future Variability and Trends. *Front. Earth Sci.* **2018**, *6*, 228. [[CrossRef](#)]
24. Brando, P.M.; Balch, J.K.; Nepstad, D.C.; Morton, D.C.; Putz, F.E.; Coe, M.T.; Silvério, D.; Macedo, M.N.; Davidson, E.A.; Nóbrega, C.C.; et al. Abrupt increases in Amazonian tree mortality due to drought-fire interactions. *Proc. Natl. Acad. Sci. USA* **2014**, *111*, 6347–6352. [[CrossRef](#)]
25. Rappaport, D.I.; Morton, D.C.; Longo, M.; Keller, M.; Dubayah, R.; Dos-Santos, M.N. Quantifying long-term changes in carbon stocks and forest structure from Amazon forest degradation. *Environ. Res. Lett.* **2018**, *13*, 065013. [[CrossRef](#)]
26. Walker, X.J.; Baltzer, J.L.; Cumming, S.G.; Day, N.J.; Ebert, C.; Goetz, S.; Johnstone, J.F.; Potter, S.; Rogers, B.M.; Schuur, E.A.G.; et al. Increasing wildfires threaten historic carbon sink of boreal forest soils. *Nature* **2019**, *572*, 520–523. [[CrossRef](#)] [[PubMed](#)]
27. Laurance, W.F.; Nascimento, H.E.M.; Laurance, S.G.; Andrade, A.; Ribeiro, J.E.L.S.; Giraldo, J.P.; Lovejoy, T.E.; Condit, R.; Chave, J.; Harms, K.E.; et al. Rapid decay of tree-community composition in Amazonian forest fragments. *Proc. Natl. Acad. Sci. USA* **2006**, *103*, 19010–19014. [[CrossRef](#)]
28. Barlow, J.; Gardner, T.A.; Lees, A.C.; Parry, L.; Peres, C.A. How pristine are tropical forests? An ecological perspective on the pre-Columbian human footprint in Amazonia and implications for contemporary conservation. *Biol. Conserv.* **2012**, *151*, 45–49. [[CrossRef](#)]
29. Pickell, P.D.; Hermosilla, T.; Frazier, R.J.; Coops, N.C.; Wulder, M.A. Forest recovery trends derived from Landsat time series for North American boreal forests. *Int. J. Remote Sens.* **2016**, *37*, 138–149. [[CrossRef](#)]
30. White, J.C.; Wulder, M.A.; Hermosilla, T.; Coops, N.C.; Hobart, G.W. A nationwide annual characterization of 25 years of forest disturbance and recovery for Canada using Landsat time series. *Remote Sens. Environ.* **2017**, *194*, 303–321. [[CrossRef](#)]
31. Andrade, R.B.; Balch, J.K.; Parsons, A.L.; Armenteras, D.; Roman-Cuesta, R.M.; Bulkan, J. Scenarios in tropical forest degradation: Carbon stock trajectories for REDD+. *Carbon Balance Manag.* **2017**, *12*, 1–7. [[CrossRef](#)]
32. Sato, L.Y.; Gomes, V.C.F.; Shimabukuro, Y.E.; Keller, M.; Arai, E.; dos-Santos, M.N.; Brown, I.F. Post-fire changes in forest biomass retrieved by airborne LiDAR in Amazonia. *Remote Sens.* **2016**, *8*, 839. [[CrossRef](#)]
33. Barlow, J.; Peres, C.A.; Lagan, B.O.; Haugaasen, T. Large tree mortality and the decline of forest biomass following Amazonian wildfires. *Ecol. Lett.* **2003**, *6*, 6–8. [[CrossRef](#)]
34. Balch, J.K.; Nepstad, D.C.; Curran, L.M.; Brando, P.M.; Portela, O.; Guilherme, P.; Reuning-Scherer, J.D.; de Carvalho, O. Size, species, and fire behavior predict tree and liana mortality from experimental burns in the Brazilian Amazon. *For. Ecol. Manag.* **2011**, *261*, 68–77. [[CrossRef](#)]
35. Feldpausch, T.R.; Jirka, S.; Passos, C.A.M.; Jasper, F.; Riha, S.J. When big trees fall: Damage and carbon export by reduced impact logging in southern Amazonia. *For. Ecol. Manag.* **2005**, *219*, 199–215. [[CrossRef](#)]
36. Marano, G.; Langella, G.; Basile, A.; Cona, F.; Michele, C.D.; Manna, P.; Teobaldelli, M.; Saracino, A.; Terribile, F. A geospatial decision support system tool for supporting integrated forest knowledge at the landscape scale. *Forests* **2019**, *10*, 690. [[CrossRef](#)]
37. Vacchiano, G.; Magnani, F.; Collalti, A. Modeling Italian forests: State of the art and future challenges. *IForest* **2012**, *5*, 113–120. [[CrossRef](#)]
38. Kumar, L.; Sinha, P.; Taylor, S.; Alqurashi, A.F. Review of the use of remote sensing for biomass estimation to support renewable energy generation. *J. Appl. Remote Sens.* **2015**, *9*, 097696. [[CrossRef](#)]
39. Keeling, H.; Phillips, O. The global relationship between forest productivity and biomass. *Glob. Ecol. Biogeogr.* **2007**, *16*, 618–631. [[CrossRef](#)]

40. Rödiger, E.; Cuntz, M.; Rammig, A.; Fischer, R.; Taubert, F.; Huth, A. The importance of forest structure for carbon fluxes of the Amazon rainforest. *Environ. Res. Lett.* **2018**, *13*, 054013. [[CrossRef](#)]
41. Fauset, S.; Gloor, M.; Fyllas, N.M.; Phillips, O.L.; Asner, G.P.; Baker, T.R.; Patrick Bentley, L.; Brienen, R.J.W.; Christoffersen, B.O.; del Aguila-Pasquel, J.; et al. Individual-Based Modeling of Amazon Forests Suggests That Climate Controls Productivity While Traits Control Demography. *Front. Earth Sci.* **2019**, *7*, 83. [[CrossRef](#)]
42. Lewis, S.L.; Brando, P.M.; Phillips, O.L.; Van Der Heijden, G.M.F.; Nepstad, D. The 2010 Amazon drought. *Science* **2011**, *331*, 554. [[CrossRef](#)] [[PubMed](#)]
43. Berenguer, E.; Ferreira, J.; Gardner, T.A.; Aragão, L.E.O.C.; De Camargo, P.B.; Cerri, C.E.; Durigan, M.; De Oliveira, R.C.; Vieira, I.C.G.; Barlow, J. A large-scale field assessment of carbon stocks in human-modified tropical forests. *Glob. Chang. Biol.* **2014**, *20*, 3713–3726. [[CrossRef](#)] [[PubMed](#)]
44. De Faria, B.L.; Brando, P.M.; Macedo, M.N.; Panday, P.K.; Soares-Filho, B.S.; Coe, M.T. Current and future patterns of fire-induced forest degradation in amazonia. *Environ. Res. Lett.* **2017**, *12*, 095005. [[CrossRef](#)]
45. Hansen, M.C.; Potapov, P.V.; Moore, R.; Hancher, M.; Turubanova, S.A.; Tyukavina, A.; Thau, D.; Stehman, S.V.; Goetz, S.J.; Loveland, T.R.; et al. High-resolution global maps of 21st-century forest cover change. *Science* **2013**, *342*, 850–853. [[CrossRef](#)] [[PubMed](#)]
46. Wheeler, D.; Guzder-Williams, B.; Petersen, R.; Thau, D. Rapid MODIS-based detection of tree cover loss. *Int. J. Appl. Earth Obs. Geoinf.* **2018**, *69*, 78–87. [[CrossRef](#)]
47. Landsberg, J.J.; Waring, R.H. A generalised model of forest productivity using simplified concepts of radiation-use efficiency, carbon balance and partitioning. *For. Ecol. Manag.* **1997**, *95*, 209–228. [[CrossRef](#)]
48. Hirsch, A.I.; Little, W.S.; Houghton, R.A.; Scott, N.A.; White, J.D. The net carbon flux due to deforestation and forest re-growth in the Brazilian Amazon: Analysis using a process-based model. *Glob. Chang. Biol.* **2004**, *10*, 908–924. [[CrossRef](#)]
49. Coops, N.C.; Waring, R.H.; Landsberg, J.J. Assessing forest productivity in Australia and New Zealand using a physiologically-based model driven with averaged monthly weather data and satellite-derived estimates of canopy photosynthetic capacity. *For. Ecol. Manag.* **1998**, *104*, 113–127. [[CrossRef](#)]
50. Collalti, A.; Prentice, I.C. Is NPP proportional to GPP? Waring’s hypothesis 20 years on. *Tree Physiol.* **2019**, *39*, 1473–1483. [[CrossRef](#)]
51. Collalti, A.; Ibrom, A.; Stockmarr, A.; Cescatti, A.; Alkama, R.; Fernández-Martínez, M.; Matteucci, G.; Sitch, S.; Friedlingstein, P.; Ciais, P.; et al. Forest production efficiency increases with growth temperature. *Nat. Commun.* **2020**. [[CrossRef](#)]
52. Waring, R.H.; Landsberg, J.J.; Williams, M. Net primary production of forests: A constant fraction of gross primary production? *Tree Physiol.* **1998**, *18*, 129–134. [[CrossRef](#)]
53. Collalti, A.; Perugini, L.; Santini, M.; Chiti, T.; Nolè, A.; Matteucci, G.; Valentini, R. A process-based model to simulate growth in forests with complex structure: Evaluation and use of 3D-CMCC Forest Ecosystem Model in a deciduous forest in Central Italy. *Ecol. Model.* **2014**, *272*, 362–378. [[CrossRef](#)]
54. Merganičová, K.; Merganič, J.; Lehtonen, A.; Vacchiano, G.; Sever, M.Z.O.; Augustynczyk, A.L.D.; Grote, R.; Kyselová, I.; Mäkelä, A.; Yousefpour, R.; et al. Forest carbon allocation modelling under climate change. *Tree Physiol.* **2019**, *39*, 1937–1960. [[CrossRef](#)]
55. Baccini, A.; Goetz, S.J.; Walker, W.S.; Laporte, N.T.; Sun, M.; Sulla-Menashe, D.; Hackler, J.; Beck, P.S.A.; Dubayah, R.; Friedl, M.A.; et al. Estimated carbon dioxide emissions from tropical deforestation improved by carbon-density maps. *Nat. Clim. Chang.* **2012**, *2*, 182–185. [[CrossRef](#)]
56. Poorter, L.; Bongers, F.; Aide, T.M.; Almeyda Zambrano, A.M.; Balvanera, P.; Becknell, J.M.; Boukili, V.; Brancalion, P.H.S.; Broadbent, E.N.; Chazdon, R.L.; et al. Biomass resilience of Neotropical secondary forests. *Nature* **2016**, *530*, 211–214. [[CrossRef](#)]
57. Chambers, J.Q.; Tribuzy, E.S.; Toledo, L.C.; Crispim, B.F.; Higuchi, N.; Dos Santos, J.; Araújo, A.C.; Kruijt, B.; Nobre, A.D.; Trumbore, S.E. Respiration from a tropical forest ecosystem: Partitioning of sources and low carbon use efficiency. *Ecol. Appl.* **2004**, *14*, 72–88. [[CrossRef](#)]
58. Collalti, A.; Marconi, S.; Ibrom, A.; Trotta, C.; Anav, A.; D’Andrea, E.; Matteucci, G.; Montagnani, L.; Gielen, B.; Mammarella, I. validation of 3D-CMCC Forest Ecosystem Model (v.5.1) against eddy covariance data for ten European forest sites. *Geosci. Model Dev.* **2016**, *9*, 479–504. [[CrossRef](#)]
59. Almeida, A.C.; Landsberg, J.J.; Sands, P.J. Parameterisation of 3-PG model for fast-growing Eucalyptus grandis plantations. *For. Ecol. Manag.* **2004**, *193*, 179–195. [[CrossRef](#)]
60. Avitabile, V.; Herold, M.; Heuvelink, G.B.M.; Lewis, S.L.; Phillips, O.L.; Asner, G.P.; Armston, J.; Ashton, P.S.; Banin, L.; Bayol, N.; et al. An integrated pan-tropical biomass map using multiple reference datasets. *Glob. Chang. Biol.* **2016**, *22*, 1406–1420. [[CrossRef](#)]
61. Saatchi, S.S.; Harris, N.L.; Brown, S.; Lefsky, M.; Mitchard, E.T.A.; Salas, W.; Zutta, B.R.; Buermann, W.; Lewis, S.L.; Hagen, S.; et al. Benchmark map of forest carbon stocks in tropical regions across three continents. *Proc. Natl. Acad. Sci. USA* **2011**, *108*, 9899–9904. [[CrossRef](#)]
62. Phillips, O.L.; Aragão, L.E.O.C.; Lewis, S.L.; Fisher, J.B.; Lloyd, J.; López-González, G.; Malhi, Y.; Monteagudo, A.; Peacock, J.; Quesada, C.A.; et al. Drought sensitivity of the amazon rainforest. *Science* **2009**, *323*, 1344–1347. [[CrossRef](#)] [[PubMed](#)]
63. Zemp, D.C.; Schleussner, C.F.; Barbosa, H.M.J.; Hirota, M.; Montade, V.; Sampaio, G.; Staal, A.; Wang-Erlandsson, L.; Rammig, A. Self-amplified Amazon forest loss due to vegetation-atmosphere feedbacks. *Nat. Commun.* **2017**, *8*, 1–10. [[CrossRef](#)]
64. Aragão, L.E.O.C.; Malhi, Y.; Roman-Cuesta, R.M.; Saatchi, S.; Anderson, L.O.; Shimabukuro, Y.E. Spatial patterns and fire response of recent Amazonian droughts. *Geophys. Res. Lett.* **2007**, *34*. [[CrossRef](#)]

65. Andela, N.; Morton, D.C.; Giglio, L.; Paugam, R.; Chen, Y.; Hantson, S.; Van Der Werf, G.R.; Anderson, J.T. The Global Fire Atlas of individual fire size, duration, speed and direction. *Earth Syst. Sci. Data* **2019**, *11*, 529–552. [[CrossRef](#)]
66. Broadbent, E.N.; Asner, G.P.; Keller, M.; Knapp, D.E.; Oliveira, P.J.C.; Silva, J.N. Forest fragmentation and edge effects from deforestation and selective logging in the Brazilian Amazon. *Biol. Conserv.* **2008**, *141*, 1745–1757. [[CrossRef](#)]
67. Harris, I.; Jones, P.D.; Osborn, T.J.; Lister, D.H. Updated high-resolution grids of monthly climatic observations—the CRU TS3.10 Dataset. *Int. J. Climatol.* **2014**, *34*, 623–642. [[CrossRef](#)]
68. Lee, H. *Climate Algorithm Theoretical Basis Document (C-ATBD): Outgoing Longwave Radiation (OLR)-Daily*. NOAA's Climate Data Record (CDR) Program, CDRP-ATBD-0526; Broadway: New York, NY, USA, 2014.
69. Hunter, M.O.; Keller, M.; Victoria, D.; Morton, D.C. Tree height and tropical forest biomass estimation. *Biogeosciences* **2013**, *10*, 8385–8399. [[CrossRef](#)]
70. Shao, G.; Stark, S.C.; de Almeida, D.R.A.; Smith, M.N. Towards high throughput assessment of canopy dynamics: The estimation of leaf area structure in Amazonian forests with multitemporal multi-sensor airborne lidar. *Remote Sens. Environ.* **2019**, *221*, 1–13. [[CrossRef](#)]
71. Rex, F.E.; Silva, C.A.; Corte, A.P.D.; Klauber, C.; Mohan, M.; Cardil, A.; da Silva, V.S.; de Almeida, D.R.A.; Garcia, M.; Broadbent, E.N.; et al. Comparison of statistical modelling approaches for estimating tropical forest aboveground biomass stock and reporting their changes in low-intensity logging areas using multi-temporal LiDAR data. *Remote Sens.* **2020**, *12*, 1498. [[CrossRef](#)]
72. Asner, G.P.; Powell, G.V.N.; Mascaró, J.; Knapp, D.E.; Clark, J.K.; Jacobson, J.; Kennedy-Bowdoin, T.; Balaji, A.; Paez-Acosta, G.; Victoria, E.; et al. High-resolution forest carbon stocks and emissions in the Amazon. *Proc. Natl. Acad. Sci. USA* **2010**, *107*, 16738–16742. [[CrossRef](#)]
73. Meyer, V.; Saatchi, S.; Ferraz, A.; Xu, L.; Duque, A.; García, M.; Chave, J. Forest degradation and biomass loss along the Chocó region of Colombia. *Carbon Balance Manag.* **2019**, *14*, 2. [[CrossRef](#)] [[PubMed](#)]
74. Aguiar, A.P.D.; Vieira, I.C.G.; Assis, T.O.; Dalla-Nora, E.L.; Toledo, P.M.; Oliveira Santos-Junior, R.A.; Batistella, M.; Coelho, A.S.; Savaget, E.K.; Aragão, L.E.O.C.; et al. Land use change emission scenarios: Anticipating a forest transition process in the Brazilian Amazon. *Glob. Chang. Biol.* **2016**, *22*, 1821–1840. [[CrossRef](#)] [[PubMed](#)]
75. Taylor, K.E.; Stouffer, R.J.; Meehl, G.A. An overview of CMIP5 and the experiment design. *Bull. Am. Meteorol. Soc.* **2012**, *93*, 485–498. [[CrossRef](#)]
76. Fonseca, M.G.; Alves, L.M.; Aguiar, A.P.D.; Arai, E.; Anderson, L.O.; Rosan, T.M.; Shimabukuro, Y.E.; de Aragão, L.E.O.E.C. Effects of climate and land-use change scenarios on fire probability during the 21st century in the Brazilian Amazon. *Glob. Chang. Biol.* **2019**, *25*, 2931–2946. [[CrossRef](#)] [[PubMed](#)]
77. Elias, F.; Ferreira, J.; Lennox, G.D.; Berenguer, E.; Ferreira, S.; Schwartz, G.; de Oliveira Melo, L.; Reis Júnior, D.N.; Nascimento, R.O.; Ferreira, F.N.; et al. Assessing the growth and climate sensitivity of secondary forests in highly deforested Amazonian landscapes. *Ecology* **2020**, *101*, e02954. [[CrossRef](#)]
78. Schwalm, C.R.; Anderegg, W.R.L.; Michalak, A.M.; Fisher, J.B.; Biondi, F.; Koch, G.; Litvak, M.; Ogle, K.; Shaw, J.D.; Wolf, A.; et al. Global patterns of drought recovery. *Nature* **2017**, *548*, 202–205. [[CrossRef](#)]
79. Engelbrecht, B.M.J.; Comita, L.S.; Condit, R.; Kursar, T.A.; Tyree, M.T.; Turner, B.L.; Hubbell, S.P. Drought sensitivity shapes species distribution patterns in tropical forests. *Nature* **2007**, *447*, 80–82. [[CrossRef](#)]
80. Saatchi, S.; Asefi-Najafabady, S.; Malhi, Y.; Aragão, L.E.O.C.; Anderson, L.O.; Myneni, R.B.; Nemani, R. Persistent effects of a severe drought on Amazonian forest canopy. *Proc. Natl. Acad. Sci. USA* **2013**, *110*, 565–570. [[CrossRef](#)]
81. Malhi, Y.; Roberts, J.T.; Betts, R.A.; Killeen, T.J.; Li, W.; Nobre, C.A. Climate change, deforestation, and the fate of the Amazon. *Science* **2008**, *319*, 169–172. [[CrossRef](#)]
82. Malhi, Y.; Doughty, C.E.; Goldsmith, G.R.; Metcalfe, D.B.; Girardin, C.A.J.; Marthews, T.R.; del Aguila-Pasquel, J.; Aragão, L.E.O.C.; Araujo-Murakami, A.; Brando, P.; et al. The linkages between photosynthesis, productivity, growth and biomass in lowland Amazonian forests. *Glob. Chang. Biol.* **2015**, *21*, 2283–2295. [[CrossRef](#)]
83. Collalti, A.; Trotta, C.; Keenan, T.F.; Ibrom, A.; Bond-Lamberty, B.; Grote, R.; Vicca, S.; Reyer, C.P.O.; Migliavacca, M.; Veroustraete, F.; et al. Thinning Can Reduce Losses in Carbon Use Efficiency and Carbon Stocks in Managed Forests Under Warmer Climate. *J. Adv. Model. Earth Syst.* **2018**, *10*, 2427–2452. [[CrossRef](#)]
84. Joetzjer, E.; Douville, H.; Delire, C.; Ciais, P. Present-day and future Amazonian precipitation in global climate models: CMIP5 versus CMIP3. *Clim. Dyn.* **2013**, *41*, 2921–2936. [[CrossRef](#)]
85. Boisier, J.P.; Ciais, P.; Ducharme, A.; Guimberteau, M. Projected strengthening of Amazonian dry season by constrained climate model simulations. *Nat. Clim. Chang.* **2015**, *5*, 656–660. [[CrossRef](#)]
86. Duffy, P.B.; Brando, P.; Asner, G.P.; Field, C.B. Projections of future meteorological drought and wet periods in the Amazon. *Proc. Natl. Acad. Sci. USA* **2015**, *112*, 13172–13177. [[CrossRef](#)]
87. Cai, W.; Borlace, S.; Lengaigne, M.; Van Rensch, P.; Collins, M.; Vecchi, G.; Timmermann, A.; Santoso, A.; McPhaden, M.J.; Wu, L.; et al. Increasing frequency of extreme El Niño events due to greenhouse warming. *Nat. Clim. Chang.* **2014**, *4*, 111–116. [[CrossRef](#)]
88. Lau, W.K.M.; Kim, K.-M. Robust Hadley Circulation changes and increasing global dryness due to CO<sub>2</sub> warming from CMIP5 model projections. *Proc. Natl. Acad. Sci. USA* **2015**, *112*, 3630–3635. [[CrossRef](#)]

89. Nepstad, D.C.; Tohver, I.M.; David, R.; Moutinho, P.; Cardinot, G. Mortality of large trees and lianas following experimental drought in an amazon forest. *Ecology* **2007**, *88*, 2259–2269. [[CrossRef](#)]
90. Poulter, B.; Hattermann, F.; Hawkins, E.; Zaehle, S.; Sitch, S.; Restrepo-Coupe, N.; Heyder, U.; Cramer, W. Robust dynamics of Amazon dieback to climate change with perturbed ecosystem model parameters. *Glob. Chang. Biol.* **2010**, *16*, 2476–2495. [[CrossRef](#)]
91. Nepstad, D.; Lefebvre, P.; Da Silva, U.L.; Tomasella, J.; Schlesinger, P.; Solórzano, L.; Moutinho, P.; Ray, D.; Benito, J.G. Amazon drought and its implications for forest flammability and tree growth: A basin-wide analysis. *Glob. Chang. Biol.* **2004**, *10*, 704–717. [[CrossRef](#)]
92. Liu, J.; Vogelmann, J.E.; Zhu, Z.; Key, C.H.; Sleeter, B.M.; Price, D.T.; Chen, J.M.; Cochrane, M.A.; Eidenshink, J.C.; Howard, S.M.; et al. Estimating California ecosystem carbon change using process model and land cover disturbance data: 1951–2000. *Ecol. Model.* **2011**, *222*, 2333–2341. [[CrossRef](#)]
93. Doughty, C.E.; Metcalfe, D.B.; Girardin, C.A.J.; Amézquita, F.F.; Cabrera, D.G.; Huasco, W.H.; Silva-Espejo, J.E.; Araujo-Murakami, A.; Da Costa, M.C.; Rocha, W.; et al. Drought impact on forest carbon dynamics and fluxes in Amazonia. *Nature* **2015**, *519*, 78–82. [[CrossRef](#)] [[PubMed](#)]
94. Yang, Y.; Saatchi, S.S.; Xu, L.; Yu, Y.; Choi, S.; Phillips, N.; Kennedy, R.; Keller, M.; Knyazikhin, Y.; Myneni, R.B. Post-drought decline of the Amazon carbon sink. *Nat. Commun.* **2018**, *9*, 1–9. [[CrossRef](#)] [[PubMed](#)]
95. De Faria, B.L.; Staal, A.; Martin, P.A.; Panday, P.K.; Castanho, A.D.; Dantas, V.L. Climate change and deforestation boost post-fire grass invasion of Amazonian forests. *bioRxiv* **2019**. [[CrossRef](#)]
96. Jolly, W.M.; Cochrane, M.A.; Freeborn, P.H.; Holden, Z.A.; Brown, T.J.; Williamson, G.J.; Bowman, D.M.J.S. Climate-induced variations in global wildfire danger from 1979 to 2013. *Nat. Commun.* **2015**, *6*, 1–11. [[CrossRef](#)] [[PubMed](#)]
97. Cardil, A.; de-Miguel, S.; Silva, C.A.; Reich, P.B.; Calkin, D.E.; Brancalion, P.H.S.; Vibrans, A.C.; Gamarra, J.G.P.; Zhou, M.; Pijanowski, B.C.; et al. Recent deforestation drove the spike in Amazonian fires. *Environ. Res. Lett.* **2020**, *15*, 121003. [[CrossRef](#)]
98. Vanderwel, M.C.; Coomes, D.A.; Purves, D.W. Quantifying variation in forest disturbance, and its effects on aboveground biomass dynamics, across the eastern United States. *Glob. Chang. Biol.* **2013**, *19*, 1504–1517. [[CrossRef](#)]
99. Jin, W.; He, H.S.; Thompson, F.R. Are more complex physiological models of forest ecosystems better choices for plot and regional predictions? *Environ. Model. Softw.* **2016**, *75*, 1–14. [[CrossRef](#)]
100. Collalti, A.; Thornton, P.E.; Cescatti, A.; Rita, A.; Borghetti, M.; Nolè, A.; Trotta, C.; Ciais, P.; Matteucci, G. The sensitivity of the forest carbon budget shifts across processes along with stand development and climate change. *Ecol. Appl.* **2019**, *29*, 1–18. [[CrossRef](#)]
101. Collalti, A.; Tjoelker, M.G.; Hoch, G.; Mäkelä, A.; Guidolotti, G.; Heskell, M.; Petit, G.; Ryan, M.G.; Battipaglia, G.; Matteucci, G.; et al. Plant respiration: Controlled by photosynthesis or biomass? *Glob. Chang. Biol.* **2020**, *26*, 1739–1753. [[CrossRef](#)]
102. Swann, A.L.S.; Hoffman, F.M.; Koven, C.D.; Randerson, J.T. Plant responses to increasing CO<sub>2</sub> reduce estimates of climate impacts on drought severity. *Proc. Natl. Acad. Sci. USA* **2016**, *113*, 10019–10024. [[CrossRef](#)]
103. Holtum, J.A.M.; Winter, K. Elevated [CO<sub>2</sub>] and forest vegetation: More a water issue than a carbon issue? *Funct. Plant Biol.* **2010**, *37*, 694–702. [[CrossRef](#)]
104. Jiang, M.; Medlyn, B.E.; Drake, J.E.; Duursma, R.A.; Anderson, I.C.; Barton, C.V.M.; Boer, M.M.; Carrillo, Y.; Castañeda-Gómez, L.; Collins, L.; et al. The fate of carbon in a mature forest under carbon dioxide enrichment. *Nature* **2020**, *580*, 227–231. [[CrossRef](#)] [[PubMed](#)]
105. Hofhansl, F.; Andersen, K.M.; Fleischer, K.; Fuchslueger, L.; Rammig, A.; Schaap, K.J.; Valverde-Barrantes, O.J.; Lapola, D.M. Amazon forest ecosystem responses to elevated atmospheric CO<sub>2</sub> and alterations in nutrient availability: Filling the gaps with model-experiment integration. *Front. Earth Sci.* **2016**, *4*, 19. [[CrossRef](#)]
106. Hubau, W.; Lewis, S.L.; Phillips, O.L.; Affum-Baffoe, K.; Beeckman, H.; Cuní-Sánchez, A.; Daniels, A.K.; Ewango, C.E.N.; Fauset, S.; Mukinzi, J.M.; et al. Asynchronous carbon sink saturation in African and Amazonian tropical forests. *Nature* **2020**, *579*, 80–87. [[CrossRef](#)]
107. Longo, M.; Keller, M.; dos-Santos, M.N.; Leitold, V.; Pinagé, E.R.; Baccini, A.; Saatchi, S.; Nogueira, E.M.; Batistella, M.; Morton, D.C. Aboveground biomass variability across intact and degraded forests in the Brazilian Amazon. *Glob. Biogeochem. Cycles* **2016**, *30*, 1639–1660. [[CrossRef](#)]
108. Longo, M.; Knox, R.G.; Medvigy, D.M.; Levine, N.M.; Dietze, M.C.; Kim, Y.; Swann, A.L.S.; Zhang, K.; Rollinson, C.R.; Bras, R.L.; et al. The biophysics, ecology, and biogeochemistry of functionally diverse, vertically and horizontally heterogeneous ecosystems: The Ecosystem Demography model, version 2.2-Part 1: Model description. *Geosci. Model. Dev. Discuss.* **2019**, *12*, 4309–4346. [[CrossRef](#)]
109. Longo, M.; Saatchi, S.; Keller, M.; Bowman, K.; Ferraz, A.; Moorcroft, P.R.; Morton, D.C.; Bonal, D.; Brando, P.; Burban, B.; et al. Impacts of Degradation on Water, Energy, and Carbon Cycling of the Amazon Tropical Forests. *J. Geophys. Res. Biogeosci.* **2020**, *125*, e2020JG005677. [[CrossRef](#)]
110. Dubayah, R.; Blair, J.B.; Goetz, S.; Fatoyinbo, L.; Hansen, M.; Healey, S.; Hofton, M.; Hurtt, G.; Kellner, J.; Luthcke, S.; et al. The Global Ecosystem Dynamics Investigation: High-resolution laser ranging of the Earth's forests and topography. *Sci. Remote Sens.* **2020**, *1*, 100002. [[CrossRef](#)]

- 
111. Potapov, P.; Li, X.; Hernandez-Serna, A.; Tyukavina, A.; Hansen, M.C.; Kommareddy, A.; Pickens, A.; Turubanova, S.; Tang, H.; Silva, C.E.; et al. Mapping global forest canopy height through integration of GEDI and Landsat data. *Remote Sens. Environ.* **2020**, *242*, 112165. [[CrossRef](#)]
  112. Duncanson, L.; Neuenschwander, A.; Hancock, S.; Thomas, N.; Fatoyinbo, T.; Simard, M.; Silva, C.A.; Armston, J.; Luthcke, S.B.; Hofton, M.; et al. Biomass estimation from simulated GEDI, ICESat-2 and NISAR across environmental gradients in Sonoma County, California. *Remote Sens. Environ.* **2020**, *242*, 111779. [[CrossRef](#)]